

## Theoretical Study of the Photodecomposition of Methyl Hg Complexes

J. A. Tossell

Department of Chemistry and Biochemistry, University of Maryland, College Park, Maryland 20742

Received: November 18, 1997; In Final Form: March 20, 1998

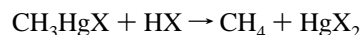
Methyl mercury, an important pollutant, decomposes photolytically when exposed to sunlight. Methyl mercury chloride has been shown to yield  $\text{CH}_3$  and  $\text{HgCl}$  radicals upon photodecomposition under UV irradiation. We have calculated spectral transition energies for a number of methylmercury species using quantum mechanical methods, specifically the Hartree–Fock method, the Moller–Plessett second order perturbation theory method (MP2), and the configuration interaction singles method using polarized double- $\zeta$  relativistic effective core potential basis sets. We find that singlet to triplet absorptions occur at lower energy than that of singlet to singlet absorptions, by about 2–3 eV. The calculated singlet to triplet (S–T) energy is much lower for 1-coordinate  $\text{CH}_3\text{Hg}^+$  than for the 2-coordinate species  $\text{CH}_3\text{HgL}$ , where  $\text{L}=\text{CH}_3^-$ ,  $\text{OH}_2$ ,  $\text{OH}^-$ ,  $\text{Cl}^-$ , or  $\text{SH}^-$ . Of the 2-coordinate species studied,  $\text{CH}_3\text{HgOH}_2^+$  and  $\text{CH}_3\text{HgSH}$  show the lowest energy S–T transitions, with calculated maxima just below 5.0 eV (at the MP2 level). They should, therefore, show significant absorption at 4.4 eV, the cutoff in the solar spectrum produced by the ozone layer. The lowest energy triplet states of these compounds are calculated to be dissociative, e.g.,  $\text{CH}_3\text{HgCl}$  decomposes to a  $\text{CH}_3$  radical and the neutral  $\text{HgCl}$  radical, while  $\text{CH}_3\text{HgOH}_2^+$  decomposes to  $\text{CH}_3$  and  $\text{HgOH}_2^+$ . The dissociation of the  $\text{CH}_3$  group can be understood by considering the compositions of the highest energy occupied and lowest energy unoccupied molecular orbitals (HOMO's and LUMO's) of the singlet states, which are Hg–C  $\sigma$ -bonding and Hg–C  $\sigma$ -antibonding, respectively. Creation of the triplet state depopulates the HOMO and populates the LUMO, greatly reducing the Hg–C bond strength. Reaction energies have also been calculated for the formation of various  $\text{CH}_3\text{HgL}$  species from  $\text{CH}_3\text{Hg}^+$  and the ligands, L. The reaction energetics indicate that  $\text{CH}_3\text{HgOH}_2^+$  and  $\text{CH}_3\text{HgOH}$  are the most important species even in the presence of appreciable  $\text{Cl}^-$  or  $\text{SH}^-$ . Therefore, the methyl Hg species decomposed by sunlight in natural water systems is probably  $\text{CH}_3\text{HgOH}_2^+$ .

### Introduction

Mercury compounds, both inorganic and organometallic, are important pollutants. Recently Sellers et al.<sup>1</sup> demonstrated that methyl Hg compounds in lake water can be decomposed by sunlight. This has important implications for the Hg budget in natural water systems. Due to the low concentrations of the methyl Hg species present and the large number of possible species in the lake water, it was impossible to determine what molecular species were actually undergoing photodecomposition. Inoko<sup>2</sup> had earlier studied the photochemistry of  $\text{CH}_3\text{-HgCl}$ , establishing that it decomposed under UV irradiation (but not sunlight) to give  $\text{CH}_3$  and  $\text{HgCl}$  radicals. Amyot et al.<sup>3</sup> have also reported increased formation of dissolved gaseous Hg upon sunlight irradiation of lake water, although the species producing the  $\text{Hg}(\text{g})$  was not identified. However, their results did establish that reduction of  $\text{Hg}^{2+}$  by  $\text{H}_2\text{O}_2$  was not an important mechanism and that the process was abiotic. Mason et al.<sup>4</sup> have addressed the more general question of the effect of Hg speciation upon its bioaccumulation and toxicity.

The photochemistry of some inorganic Hg compounds has been treated theoretically by Stromberg et al.<sup>5,6</sup> Due to the strong complexing which is thought to occur between Hg and S, much of their attention was focused on bisulfide complexes, particularly upon their photochemistry in the visible and near UV ranges. They found transitions below 4.4 eV (the high energy limit of the solar spectrum, due to absorption by atmospheric ozone, ref 7) for  $\text{Hg}(\text{SH})_2$ , although all the

symmetry- and spin-allowed transitions were calculated to occur at higher energy. In heavy element compounds, such as those of Hg, spin–orbit coupling effects may be large enough that spin-forbidden transitions acquire appreciable intensity. Barone et al.<sup>8</sup> studied some methyl Hg compounds theoretically, concentrating upon the ease of Hg–C bond rupture upon the addition of mineral acids, i.e., the reaction



and were able to explain the easier cleavage of the C–Hg bond when L actually consisted of three  $\text{PH}_3$  groups. The effect of relativity upon coordination number in Hg compounds has recently been studied by Kaupp and Schnerring,<sup>9</sup> and some general considerations relating to the effects of relativity upon preferred coordination number and structure type were given previously by Tossell and Vaughan.<sup>10</sup>

This study is a continuation of a theoretical program aimed at elucidating the speciation of heavy metals in solution. Similar methods have been previously applied to Zn compounds,<sup>11</sup> Cd compounds,<sup>12</sup> and Au compounds.<sup>13</sup>

### Theoretical Methods Used

We use the traditional methods of molecular quantum chemistry, specifically the ab initio self-consistent-field Hartree–Fock method, as described in Hehre et al.<sup>14</sup> The basis sets employed in the expansion of the molecular orbitals are of the relativistic effective core potential type, those designed either

**TABLE 1: Comparison of Calculated Structure of CH<sub>3</sub>HgCl with Previous Calculations and with Experimental Values<sup>a</sup>**

method	R(Hg–Cl)	R(Hg–C)
polarized SBK Hartree–Fock	2.371	2.127
polarized SBK MP2	2.341	2.099
MP2 (Barone et al., ref 8)	2.344	2.101
MP2 with <i>f</i> polarization functions (Barone et al., ref 8)	2.302	2.084
exptl from gas phase microwave	2.282	2.061

<sup>a</sup> Distances are given in Å.

by Stevens, Basch, and Krauss (SBK, ref 15) or by Hay and Wadt (LANL2DZ, ref 16). In each case, single *d* polarization functions have been added to the ligand atoms (except H). We have used the quantum chemical software GAMESS (Schmidt et al.<sup>17</sup>) and GAUSSIAN94 (Frisch et al.<sup>18</sup>). In addition to the Hartree–Fock calculations we have carried out Moller–Plesset second order correlation energy calculations (MP2, ref 19) and configuration interaction singles calculations of both singlet and triplet excitation energies (CIS, ref 20).

## Results

Structural results for CH<sub>3</sub>HgCl obtained using polarized SBK basis sets at the HF and MP2 levels are compared with previous calculations and with the experimental values in Table 1. It is clear that to accurately reproduce the experimental structure (obtained in the gas-phase, using microwave spectroscopy) we must use rather high-level methods and large basis sets. However, the polarized SBK MP2 results are not too far from experimental values, and we have therefore done most of our work at this level. Energies for singlet to triplet excitation at the Hartree–Fock level and at the MP2 level (using MP2 optimized geometries) are presented in Table 2 for all the compounds studied. In Table 3 we compare excitation energies calculated at the Hartree–Fock and CIS levels for some of the compounds. Reaction energetics at the Hartree–Fock SCF level, with corrections for hydration of the ions, are presented in Table 4. Additional correction terms in the energy and free energy for the reaction of CH<sub>3</sub>HgCl with OH<sup>–</sup> to give CH<sub>3</sub>HgOH and Cl<sup>–</sup> are given in Table 5. Calculated and experi-

mental IR stretching energies for some of the molecules studied are reported in Table 6.

The first general observation from the data in Table 2 is that 1-coordinate CH<sub>3</sub>Hg<sup>+</sup> shows its singlet to triplet transition at lower energy than any of the 2-coordinate species. However, addition of a H<sub>2</sub>O molecule to CH<sub>3</sub>Hg<sup>+</sup> is exothermic by about 30 kcal/mol (see Table 4 below), so we would expect that 1-coordinate CH<sub>3</sub>Hg<sup>+</sup> could not actually exist in aqueous solution. There is also a general correlation between short Hg–C distances in the complex and large S–T energies, as seen in comparing CH<sub>3</sub>Hg<sup>+</sup> (with Hg–C distance of 2.228 Å and S–T energy of 2.05 eV) and (CH<sub>3</sub>)<sub>2</sub>Hg (with Hg–C distance of 2.152 Å and S–T energy of 4.81 eV). There is also a strong tendency for dissociation in the lowest energy triplet state of CH<sub>3</sub>HgL, with CH<sub>3</sub> radicals being produced. Similarly, the triplet states of HgCl<sub>2</sub> and Hg(SH)<sub>2</sub> are dissociative, producing Cl or SH radicals

We can understand this dissociation in electronic structural terms by looking at the HOMO and LUMO of the singlet state of CH<sub>3</sub>HgOH<sub>2</sub><sup>+</sup>, as shown in Figure 1. The HOMO is clearly *bonding* between the Hg and the CH<sub>3</sub> group, and the LUMO is Hg–C *antibonding*. The qualitative change from the singlet to the triplet state is that the Hg–C bonding MO becomes only half occupied, while at the same time the Hg–C antibonding MO also becomes half occupied. This leads to a large reduction in the strength of the Hg–C bond, leading to the dissociation of the CH<sub>3</sub> radical during the geometry optimization. The LUMO of the singlet is also somewhat Hg–L antibonding so that its partial occupation in the triplet state will also increase the Hg–L distance. Figure 1 also suggests an explanation for the trend in S–T energies. Since producing the triplet from the singlet essentially requires a  $\sigma$ -bonding to  $\sigma$ -antibonding orbital excitation, this excitation will increase in energy as the bonding and antibonding character of the MO's increases, which will occur when the Hg–C distance decreases. This interpretation is consistent with the relationship between Hg–C distances and S–T energies mentioned above.

There is generally good agreement between the results of the Hartree–Fock and the CI singles calculations for the CH<sub>3</sub>Hg species in terms of both triplet energies (excited singlet energies

**TABLE 2: Calculated Properties of LHgL' Complexes<sup>a</sup>**

LHgL'	$\Delta E_{S-T}$		R(Hg–L)		R(Hg–L')		changes in Hg–L and Hg–L' distances upon S–T excitation
	HF <sup>a</sup>	MP2	HF	MP2	HF	MP2	
CH <sub>3</sub> Hg <sup>+</sup>	2.05 (1.09)	3.10	2.228	2.166			HF and MP2: Hg–C elongates by about 1.0 Å
(CH <sub>3</sub> ) <sub>2</sub> Hg	4.81 (1.36)	5.80	2.152	2.127	2.152	2.127	HF and MP2: both R(Hg–C) elongate by >1.0 Å
CH <sub>3</sub> HgOH <sub>2</sub> <sup>+</sup>	3.97 (1.56)	4.97	2.140	2.101	2.299	2.248	HF and MP2: CH <sub>3</sub> leaves
CH <sub>3</sub> HgOH	~5.9 <sup>b</sup>		2.117	2.096	2.024	2.028	HF and MP2: CH <sub>3</sub> and OH leave
CH <sub>3</sub> HgCl	5.41 (1.84)	6.04	2.127	2.099	2.371	2.341	HF and MP2: CH <sub>3</sub> leaves
CH <sub>3</sub> HgSH	5.16 (1.80)	4.98	2.139	2.113	2.413	2.383	HF and MP2: CH <sub>3</sub> leaves
HgCl <sub>2</sub>	6.36 (2.50)	5.18	2.327	2.304	2.327	2.304	HF and MP2: one Cl leaves
Hg(SH) <sub>2</sub>	5.47 (2.05)	4.26	2.392	2.366	2.392	2.366	HF and MP2: one SH leaves

<sup>a</sup> Both vertical and adiabatic (in parentheses) energies are given for the singlet to triplet excitation at the HF level. All energies are from Hartree–Fock or MP2 calculations using the polarized SBK basis and are measured in eV. <sup>b</sup> HF did not converge at geometry of singlet.

**TABLE 3: Comparison of Hartree–Fock and Configuration Interaction Singles (CIS) Excitation Energies (Evaluated at HF Geometries) and MP2 Excitation Energies (Evaluated at MP2 Geometries) for CH<sub>3</sub>Hg<sup>+</sup>, CH<sub>3</sub>HgCl, CH<sub>3</sub>HgOH<sub>2</sub><sup>+</sup>, and HgCl<sub>2</sub> with Available Experimental Data**

molecule	CH <sub>3</sub> Hg <sup>+</sup>	CH <sub>3</sub> HgCl	CH <sub>3</sub> HgSH	CH <sub>3</sub> HgOH <sub>2</sub> <sup>+</sup>	HgCl <sub>2</sub>
$\Delta E_{S-T}$ (HF)	2.05	5.41	5.16	3.97	6.36
$\Delta E_{S-T}$ (MP2)	3.10	6.04	4.98	4.97	5.18
$\Delta E_{S-T}$ (CIS)	2.05, 6.02, 6.02	5.43, 6.73, 6.73 (5.68, 6.88, 6.99 <sup>a</sup> )	5.20, 5.43, 5.99	3.97, 6.17, 6.36	5.55, 5.55, 5.89
$\Delta E_{S-S}$ (CIS)	5.11, 7.77, 7.77	7.29, 7.29, 7.63 (7.49, 7.71, 7.71 <sup>a</sup> )	6.07, 6.45, 6.58	6.64, 7.70, 7.89	6.05, 6.05, 6.67
exptl excitation energies		absorbs in UV, $\Delta E > 3$ eV			absorbs at 6.2 eV

<sup>a</sup> Evaluated at MP2 optimized geometry.

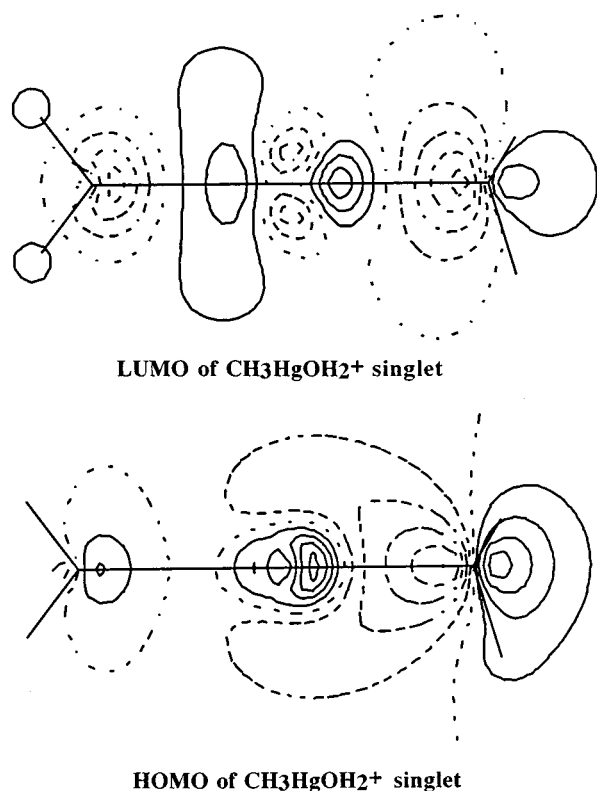


**Figure 1.** Plots of the HOMO and LUMO of  $\text{CH}_3\text{HgOH}_2^+$  in the singlet state at the polarized SBK HF optimized geometry.  $\text{H}_2\text{O}$  is on the left, Hg is at the center, and the  $\text{CH}_3$  group is on the right.

**TABLE 4: Calculated Reaction Energies at the Polarized SBK HF Level for Aqueous Solution (Unless Otherwise Noted)<sup>a</sup>**

reaction	$\Delta E^b$
(1) $\text{CH}_3\text{Hg}^+ + \text{H}_2\text{O} \rightarrow \text{CH}_3\text{HgOH}_2^+$ (gas phase)	-29.6
(2) $\text{CH}_3\text{HgCl} + \text{OH}^- \rightarrow \text{CH}_3\text{HgOH} + \text{Cl}^-$	-20.0
(3) $\text{CH}_3\text{HgOH} + \text{SH}^- \rightarrow \text{CH}_3\text{HgSH} + \text{OH}^-$	+126.6
(4) $\text{CH}_3\text{HgOH}_2^+ \rightarrow \text{CH}_3\text{HgOH} + \text{H}^+$	+32.6
(5) $\text{CH}_3\text{HgOH}_2^+ + \text{OH}^- \rightarrow \text{CH}_3\text{HgOH} + \text{H}_2\text{O}$	-72.8
(6) $\text{CH}_3\text{HgOH}_2^+ + \text{SH}^- \rightarrow \text{CH}_3\text{HgSH} + \text{H}_2\text{O}$	+117.3
(7) $\text{CH}_3\text{HgSH} + \text{OH}^- \rightarrow \text{CH}_3\text{HgS} + \text{H}_2\text{O}$	-138.0
(8) $2\text{HgCl} \rightarrow \text{HgCl}_2 + \text{Hg}$ (gas phase)	-41.8
(9) $\text{CH}_3 + \text{HgCl} \rightarrow \text{CH}_3\text{Cl} + \text{Hg}$	-43.1

<sup>a</sup> Hydration energies calculated as explained in the text. <sup>b</sup> Energies in kcal/mol.

**TABLE 5: Additional Terms Involved in the Solution Energetics of the Reaction:  $\text{CH}_3\text{HgCl} + \text{OH}^- \rightarrow \text{CH}_3\text{HgOH} + \text{Cl}^-$ <sup>a</sup>**

method	$\Delta E$
Hartree-Fock, gas phase	-45.1
MP2 at Hartree-Fock geometry, gas phase	-45.0
MP2 at reoptimized geometry, gas phase	-45.5
reoptimized MP2 plus zero-point vibrational energy	-43.4
reoptimized MP2 plus enthalpy corrections at 298 K	-42.6
above with experimental hydration energies of $\text{OH}^-$ and $\text{Cl}^-$	-19.1
above with calculated hydration energies of $\text{CH}_3\text{HgOH}$ and $\text{Cl}^-$	-17.9
$\text{CH}_3\text{HgCl}$ (from supermolecule calculations) added	
experimental enthalpy difference at 298 K from ref 23	-2.5

<sup>a</sup> Energies in kcal/mol.

cannot be evaluated with the HF method) and changes in geometry compared to the ground state, although for  $\text{HgCl}_2$  the discrepancies are somewhat larger. However, using the CIS method we can get more complete information on the energies of several singlet-singlet and singlet-triplet transitions, not just the lowest energy S-T transition, and we can determine the

**TABLE 6: Calculated Unscaled and Experimental (in Parentheses)<sup>a</sup> IR Stretching Frequencies for Some  $\text{CH}_3\text{HgL}$  Compounds**

molecule	Hg-C stretch <sup>b</sup>	Hg-L stretch <sup>b</sup>
$\text{CH}_3\text{Hg}^+$	385	
$\text{CH}_3\text{HgCl}$	543, 540 <sup>c</sup> (556)	337, 333 <sup>b</sup> (334)
$\text{CH}_3\text{HgOH}$	599 (577)	532 (511)
$\text{CH}_3\text{HgOH}_2^+$	498 (463)	286
$\text{CH}_3\text{HgSH}$	564	355

<sup>a</sup> Experimental values from ref 22. <sup>b</sup> Frequencies in  $\text{cm}^{-1}$ . <sup>c</sup> From ref 7.

equilibrium geometries for the various states. The S-S transition energies are always about 2-3 eV higher than the S-T energies. Therefore, the singlet transition energies, even for  $\text{CH}_3\text{Hg}^+$ , lie well into the UV. Thus, if decomposition occurs under sunlight irradiation, it must occur through the creation of the lowest energy triplets.

The HF and CIS methods represent similar levels of approximation for the lowest energy triplet and give results which are often very close. Since the HF (actually UHF) results allow the MO's to change in response to orbital occupation, they are probably somewhat better. For  $\text{HgCl}_2$ , the HF and CIS methods give lowest S-T energies, differing by about 0.8 eV. The MP2 S-T excitation energies for the lowest triplets are, in principle, of higher accuracy, because first, the MP2-optimized geometries are in better agreement with experiment and second, the MP2 method incorporates correlation effects not present in HF or CIS. We find, in general, that about one-fourth of the difference between the HF and MP2 results arises from the indirect effect of the differing bond distances, and the other three-fourths arises from the difference of the HF and MP2 energy expressions. Similarly, the change in CIS energy for the lowest triplet state using the MP2 rather than the HF geometry is generally about one-fourth of the difference of HF and MP2 energies.

We can gauge the accuracy of our results by comparing them with the experimental values for  $\text{HgCl}_2$ . Its absorption spectrum<sup>21</sup> has a shoulder at about 5.1 eV and a maximum at about 6.2 eV, with an absorption edge extending down to about 4.6 eV. No detailed assignment of this spectrum has been made, but a reasonable interpretation would assign the shoulder to the lowest S-T transition and the maximum to the lowest S-S transition. These values are in reasonable agreement with those from the CIS calculations shown in Table 3. The HF S-T energy is somewhat larger but still reasonably close to the experimental values. We have also carried out CIS calculations for  $\text{Hg}(\text{SH})_2$ , obtaining energies of 4.60 and 5.18 eV for the lowest energy triplet and singlet transitions, respectively, in reasonable agreement with the values of 4.3 and 4.7 eV from the complete-active-space SCF calculations of ref 6.

To determine what  $\text{CH}_3\text{HgL}$  species will be present in natural waters, we need to have some knowledge of the energetics of their formation reactions. In Table 4 we present some reaction energies calculated at the Hartree-Fock level using the method of Rashin and Honig<sup>22</sup> to evaluate the hydration energies of the small cations and anions. The stability constants tabulated by Smith and Martell<sup>23</sup> can then be used to determine reaction free energies to be compared with the calculated energetics. Reaction 1 in this Table is the addition of  $\text{H}_2\text{O}$  to  $\text{CH}_3\text{Hg}^+$  in the gas phase and is strongly endothermic. It is not really clear how to generalize this reaction to aqueous solution, since the first  $\text{H}_2\text{O}$  added is part of the first hydration sphere. For reactions 2 and 3, we need only the hydration energies of the small anions  $\text{OH}^-$ ,  $\text{Cl}^-$ , and  $\text{SH}^-$ , for which experimental values are given in ref 22. Our conclusion that  $\text{CH}_3\text{HgOH}$  is more

stable than  $\text{CH}_3\text{HgCl}$  is in accord with experimental values, although the free energy change for reaction 2 obtained from the  $\log K$  values in ref 23 is only about  $-5.2$  kcal/mol, rather than the  $-20.0$  kcal/mol we calculate. Likewise we calculate  $\text{CH}_3\text{HgOH}$  to be more stable than  $\text{CH}_3\text{HgSH}$ . To refine our energetics for reaction 2, we have considered some other smaller terms in the free energy change (use of MP2 rather than Hartree–Fock energies, hydration of the neutral molecules, zero-point vibrational energy corrections, etc.), but these change the result very little, as shown in Table 5. By far the largest correction term to the gas-phase result is the difference of hydration energies of  $\text{OH}^-$  and  $\text{Cl}^-$ . To estimate hydration energies for the larger complexes, both ionic and neutral, we have performed supermolecule and polarizable continuum calculations with six  $\text{H}_2\text{O}$  molecules surrounding the Hg complex. The general energetic effects observed are summarized below:

process	stabilization (kcal/mol)
hydration of neutral $\text{CH}_3\text{HgL}$	about 15
hydration of neutral $\text{HgCl}_2$	about 27
addition of one $\text{H}_2\text{O}$ to $\text{CH}_3\text{Hg}^+$	about 30
addition of five more $\text{H}_2\text{O}$ to $\text{CH}_3\text{HgOH}_2^+$	about 47
Born electrostatic term for $\text{CH}_3\text{Hg}(\text{H}_2\text{O})_6^+$	about 38

Evaluation of the energetics for the other reactions in Table 4 requires that the Born electrostatic terms be considered. Assuming that such terms are of about the same magnitude for all  $\text{CH}_3\text{HgL}$  ions with a charge magnitude of 1 yields the reaction energies in Table 4. On the basis of the energetics in Table 4, we would expect  $\text{CH}_3\text{HgOH}_2^+$  and  $\text{CH}_3\text{HgOH}$  to be the main species present.

Once the methyl Hg species has been photolyzed, other reactions can occur exothermically. For example, as shown in Table 4, two  $\text{HgCl}$  radicals can react exothermically in a disproportionation step to produce  $\text{HgCl}_2 + \text{Hg}$ . The  $\text{CH}_3^-$  and  $\text{HgCl}^-$  radicals can also react to produce  $\text{CH}_3\text{Cl}$  and  $\text{Hg}$ . Either process would produce elemental Hg.

If the Hg species photolyzing is indeed  $\text{CH}_3\text{HgOH}_2^+$ , it may be possible to identify it by IR or by NMR. The IR spectra of  $\text{CH}_3\text{HgL}$  complexes, including those with  $\text{L} = \text{Cl}^-$ ,  $\text{OH}^-$ , and  $\text{H}_2\text{O}$ , have been studied by Goggin et al.<sup>24</sup> In Table 6 we compare our calculated Hg–C and Hg–L stretching frequencies with their results and with those of Barone et al.<sup>8</sup> As noted by Barone et al., the comparison is better if we use unscaled calculated frequencies, rather than using frequencies scaled down by the 0.9 factor commonly used with Hartree–Fock calculations. As we saw in Table 1, our bond distances are longer than the experimental values at the Hartree–Fock level, rather than smaller, as for main group molecules. Therefore we do not have the exaggeration of force constants common at the Hartree–Fock level.<sup>14</sup> Note that our assignment differs from that of Goggin et al. for  $\text{CH}_3\text{HgOH}_2^+$ , for which we find the Hg–O stretching frequency to be quite low. The feature they assign as a Hg–C stretch at a frequency of  $570\text{ cm}^{-1}$  we find to be primarily a  $\text{CH}_3$  deformation mode. The surprising fact that both stretching frequencies are higher in  $\text{CH}_3\text{HgOH}$  than in  $\text{CH}_3\text{HgCl}$  arises from some mixing of Hg–C and Hg–O motions within the modes, making them somewhat like the symmetric and antisymmetric stretches of an  $\text{AB}_2$  molecule like  $\text{HgCl}_2$ . These two normal vibrational modes of  $\text{CH}_3\text{HgOH}$  are shown in Figure 2.

<sup>13</sup>C NMR is also a potential technique for identification of such species. Studies of  $\text{CH}_3\text{HgL}$  compounds<sup>25</sup> show significant changes in C shielding as L changes, but we presently do not

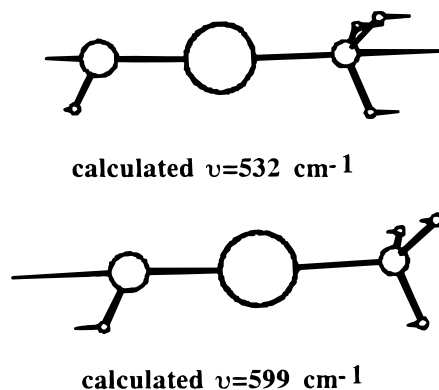


**Figure 2.** Plots of the two vibrational normal modes of  $\text{CH}_3\text{HgOH}$  involving Hg–O and Hg–C stretching. The OH group is on the left and the  $\text{CH}_3$  group on the right. The lengths of the arrows are proportional to the nuclear displacements within the normal modes.

have reliable methods to calculate these NMR shifts or to interpret them. For example, it is observed that the C in  $(\text{CH}_3)_2\text{Hg}$  is deshielded with respect to that in  $\text{CH}_3\text{Hg}^+$ , which was explained<sup>25</sup> in terms of a smaller average excitation energy in  $(\text{CH}_3)_2\text{Hg}$ . However, we have seen that the excitation energies are actually considerably larger in  $(\text{CH}_3)_2\text{Hg}$  than in  $\text{CH}_3\text{Hg}^+$ , so the energy difference alone cannot be the explanation for the shielding trend.

## Conclusions

Our results are consistent with the presence of  $\text{CH}_3\text{HgOH}_2^+$  and  $\text{CH}_3\text{HgOH}$  as the main methyl Hg complexes in natural water systems. Under conditions of appreciable  $\text{Cl}^-$  or  $\text{SH}^-$  concentration, the species  $\text{CH}_3\text{HgCl}$  and  $\text{CH}_3\text{HgSH}$  could also be present.  $\text{CH}_3\text{HgOH}_2^+$  is calculated to show a singlet–triplet excitation maximum not far above the energy limit of 4.4 eV for solar radiation imposed by the ozone layer. Given a reasonable width for this transition, it could certainly be excited by sunlight. The triplet states which are formed dissociate to produce  $\text{CH}_3$  radicals and  $\text{Hg(I)L}$  radicals which subsequently disproportionate or react with  $\text{CH}_3$  to yield free Hg.

**Acknowledgment.** This work was supported by DOE grant DE-FG02-94ER14467.

## References and Notes

- (1) Sellers, P.; Kelly, C. A.; Rudd, J. W. M.; MacHutchon, A. R. *Nature* **1996**, *380*, 694–697.
- (2) Inoko, M. *Environ. Pollut. (Series B)* **1981**, *2*, 3–10.
- (3) Amyot, M.; Mierle, G.; Lean, D. R. S.; McQueen, D. J. *Environ. Sci. Technol.* **1994**, *28*, 2366–2371.
- (4) Mason, R. P.; Reinfelder, J. R.; Morel, F. M. M. *Environ. Sci. Technol.* **1996**, *30*, 1835–1845.
- (5) Stromberg, D.; Gropen, O.; Wahlgren, U. *Chem. Phys.* **1989**, *133*, 207–219.
- (6) Stromberg, D.; Stromberg, A.; Wahlgren, U. *Water, Air, Soil Poll.* **1991**, *56*, 681–695.
- (7) Leighton, P. A. *Photochemistry of Air Pollution*; Academic Press, New York, 1961.
- (8) Barone, V.; Bencini, A.; Totti, F.; Uytterhoeven, M. G. *J. Phys. Chem.* **1995**, *99*, 12743–12750.
- (9) Kaupp, M.; Schnering, H. G. *Inorg. Chem.* **1994**, *33*, 2555–2564.
- (10) Tossell, J. A.; Vaughan, D. J. *Inorg. Chem.* **1981**, *20*, 3333–3339.
- (11) Tossell, J. A. *J. Phys. Chem.* **1991**, *95*, 366–371.
- (12) Tossell, J. A.; Vaughan, D. J. *Geochim. Cosmochim. Acta* **1993**, *57*, 1935–1945.
- (13) Tossell, J. A. *Geochim. Cosmochim. Acta* **1996**, *60*, 17–29.
- (14) Hehre, W. J.; Radom, L.; Schleyer, P. v. R.; Pople, J. A. *Ab Initio Molecular Orbital Theory*; Wiley: New York, 1986.
- (15) Stevens, W. J.; Krauss, M.; Basch, H.; Jansen, P. G. *Can. J. Chem.* **1992**, *70*, 612.

- (16) Hay, P. J.; Wadt, W. R. *J. Chem. Phys.* **1985**, *82*, 270–283.
- (17) Schmidt, M. W.; Baldrige, K. K.; Boatz, J. A.; Elbert, S. T.; Gordon, M. S.; Jensen, J. H.; Koseki, S.; Matsunaga, N.; Nguyen, K. A.; Su, S. J.; Windus, T. L.; Dupuis, M.; Montgomery, J. A. *J. Computat. Chem.* **1993**, *14*, 1347.
- (18) Frisch, M. J.; Trucks, G. W.; Schlegel, H. B.; Gill, P. M. W.; Johnson, B. G.; Wong, M. W.; Foresman, J. B.; Robb, M. A.; Head-Gordon, M.; Replogle, E. S.; Gomperts, R.; Andres, J. L.; Raghavachari, K.; Binkley, J. S.; Gonzalez, C.; Martin, R. L.; Fox, D. J.; DeFrees, D. J.; Baker, J.; Stewart, J. J. O.; Pople, J. A. GAUSSIAN94, Rev. B.3, Gaussian, Inc.: Pittsburgh, PA.
- (19) Pople, J. A.; Binkley, J. S.; Seeger, R. *Int. J. Quantum Chem. Symp.* **1976**, *10*, 1.
- (20) Foresman, J. B.; Head-Gordon, M.; Pople, J. A.; Frisch, M. J. *J. Phys. Chem.* **1992**, *96*, 135.
- (21) Templet, P.; McDonald, J. R.; McGlynn, S. P. *J. Chem. Phys.* **1972**, *56*, 5746.
- (22) Rashin, A. A.; Honig, B. *J. Phys. Chem.* **1985**, *89*, 5588–5593.
- (23) Smith, R. M.; Martell, A. E. *Critical Stability Constants, Vol. 4: Inorganic Complexes*; Plenum Press: New York, 1976.
- (24) (a) Goggin, P. L.; Woodward, L. A. *J. Chem. Soc., Faraday Trans.* **1960**, *56*, 1591–1596. (b) Goggin, P. L.; Woodward, L. A. *J. Chem. Soc., Faraday Trans.* **1962**, *58*, 1495–1502. (c) Goggin, P. L.; Woodward, L. A. *J. Chem. Soc., Faraday Trans.* **1966**, *62*, 1423–1430.
- (25) Brown, A. J.; Howarth, O. W.; Moore, P. *J. Chem. Soc., Dalton Trans.* **1976**, 1589–1592.